Non-Fermi-liquid behavior in quantum impurity models with superconducting channels

Rok Žitko[1,2] and Michele Fabrizio[3]
[1]*Jožef Stefan Institute, Jamova 39, SI-1000 Ljubljana, Slovenia*
[2]*Faculty of Mathematics and Physics, University of Ljubljana, Jadranska 19, SI-1000 Ljubljana, Slovenia*
[3]*International School for Advanced Studies (SISSA), and CNR-IOM Democritos, Via Bonomea 265, I-34136 Trieste, Italy*
(Received 24 June 2016; revised manuscript received 3 November 2016; published 16 February 2017)

We study how the non-Fermi-liquid nature of the overscreened multichannel Kondo impurity model affects the response to a BCS pairing term that, in the absence of the impurity, opens a gap Δ. We find that the low-energy spectrum in the limit $\Delta \to 0$ actually does not correspond to the spectrum strictly at $\Delta = 0$. In particular, in the two-channel Kondo model, the $\Delta \to 0$ ground state is an orbitally degenerate spin singlet, while it is an orbital singlet with a residual spin degeneracy at $\Delta = 0$. In addition, there are fractionalized spin-1/2 subgap excitations whose energy in units of Δ tends toward a finite and universal value when $\Delta \to 0$, as if the universality of the anomalous power-law exponents that characterize the overscreened Kondo effect turned into universal energy ratios when the scale invariance is broken by $\Delta \neq 0$. This intriguing phenomenon can be explained by the renormalization flow toward the overscreened fixed point and the gap cutting off the orthogonality catastrophe singularities. We also find other non-Fermi-liquid features at finite Δ: the local density of states lacks coherence peaks, the states in the continuum above the gap are unconventional, and the boundary entropy is a nonmonotonic function of temperature. The persistent subgap excitations are characteristic of the non-Fermi-liquid fixed point of the model, and thus depend on the impurity spin and the number of screening channels.

DOI: 10.1103/PhysRevB.95.085121

I. INTRODUCTION

The density of states (DOS) $\rho(\omega)$ of a conventional BCS s-wave superconductor has a gap Δ and coherence peaks above it, $\rho(\omega) = \rho_0 \mathrm{Re}\,\omega/\sqrt{\omega^2 - \Delta^2}$, where ρ_0 is the normal-state DOS. This remains true also in the presence of disorder and impurities that maintain time-reversal invariance [1]. By contrast, magnetic impurities may induce additional states inside the gap by binding Bogoliubov quasiparticles through the exchange coupling J [2–6]. The bound-state energies depend on the interplay of Kondo screening, the superconducting proximity effect, and spin-orbit coupling [7–9], and they are measurable in hybrid superconductor-semiconductor nanostructures [10–12] and adsorbed magnetic atoms or molecules [13–15]. In the limit of a small gap, $\Delta \to 0$, the subgap states induced by impurities that are Kondo-screened below the Kondo temperature T_K (and hence effectively nonmagnetic) move toward the gap edges and merge with the coherence peaks [16–23], because the weak superconducting pairing ($\Delta \ll T_K$) perturbs a system that was formerly in a local Fermi liquid (FL) state [24]. The effect of the impurity on the bulk electrons is thus fully accounted for by the quasiparticle scattering phase shifts resulting from the Kondo effect ($\pi/2$ in the deep Kondo limit) [25]. A similar scenario occurs in the case of underscreen local moments, which have a residual local moment that is, however, asymptotically decoupled from the rest of the system; such systems are known as singular Fermi liquids [26,27], and they occur when the number of screening channels k is lower than twice the impurity spin, $2S$.

There is, however, another class of quantum impurities that are Kondo-overscreened because the number of screening channels exceeds twice the impurity spin, $k > 2S$ [28–33]. Such overcompensation has been experimentally demonstrated for the two-channel Kondo model ($k = 2$, $S = 1/2$) in artificial semiconductor quantum dot devices [34–39]. The resulting states are non-Fermi-liquids (NFLs) [29,40] with excitation spectra that deviate significantly from the FL paradigm, but they can still be described in terms of appropriate boundary conformal field theories (CFTs) [41–46], and they can be solved exactly using the Bethe ansatz [47–49]. When a small gap is opened in the contacts of such systems, the superconducting state thus emerges out of a non-Fermi-liquid. Two related questions arise: (i) What is the nature of the excitations forming the continuum above the gap? (ii) Can the subgap states be interpreted as bound states of NFL excitations?

In this work, the problem is studied using the numerical renormalization-group (NRG) technique [16,50–54] and analytical arguments. For the two-channel Kondo (2CK) model [55] in the limit $\Delta \to 0$, we find surprisingly that the low-energy spectrum does not reproduce that at $\Delta = 0$: the ground state (GS) is a doubly degenerate spin singlet, while two $S = 1/2$ subgap Shiba states become degenerate with a *universal dimensionless energy ratio*

$$\epsilon^* \equiv E^*/\Delta \approx 0.5983. \tag{1}$$

In other words, even in the $\Delta \to 0$ limit these bound states do not merge with the continuum. The GS is connected with the excitations at the rescaled energy 1/8 in the boundary CFT of the $\Delta = 0$ case, while the excited subgap states emerge out of the energy 0 and 1/2 states [41,42,56–59]. The excitations above the gap have NFL degeneracies and spacing, and there are no coherence peaks in the impurity DOS. When the NFL regime is disrupted by breaking the channel degeneracy [29,56,60–62], the subgap states do move toward the gap edge, and the coherence peaks are restored when the FL-NFL crossover scale T^* exceeds Δ.

II. MODEL

We consider the Hamiltonian $H = \sum_{i=1}^{k} J_i\, \mathbf{s}_i \cdot \mathbf{S} + H_i$, where

$$H_i = \sum_{\mathbf{k}\sigma} \epsilon_{\mathbf{k}}\, c^\dagger_{i,\mathbf{k}\sigma} c_{i,\mathbf{k}\sigma} + \sum_{\mathbf{k}} (\Delta\, c^\dagger_{i,\mathbf{k}\uparrow} c^\dagger_{i,-\mathbf{k}\downarrow} + \mathrm{H.c.}), \tag{2}$$

i.e., a k-channel Kondo model [29] with each channel described by a BCS mean-field Hamiltonian with fixed Δ. J_i is the exchange coupling, $\mathbf{s}_i$ is the spin density of channel-i electrons at the position of the impurity, $\mathbf{S}$ is the impurity spin-S operator, and finally $c^\dagger_{i,k\sigma}$ creates an electron in channel-i with momentum $\mathbf{k}$, spin σ, and energy $\epsilon_\mathbf{k}$. The continuum has a flat DOS with half-bandwidth D, i.e., $\rho_0 = 1/2D$. The Kondo scale for small exchange coupling is $T_K \approx \exp(-1/\rho_0 J_{\rm avg})$, where $J_{\rm avg} = \sum_i J_i/k$ [63]. If J_i are nonequal, there is another relevant scale T^* that grows as a power law with the difference between the two largest J_i [55]. For $\Delta = 0$, the system has NFL properties for $T^* < T < T_K$ and crosses over to a FL GS for $T < T^*$. For $\Delta \neq 0$, we use the NRG to compute the finite-size excitation spectra, thermodynamic properties, and the T-matrix spectral function (impurity DOS).

III. PERSISTENT SUBGAP STATES

A. Two-channel Kondo model

The discrete (subgap) part of the excitation spectrum for the 2CK model with $J_1 = J_2 = J$ is shown in Fig. 1(a) at a constant gap Δ as a function of the dimensionless coupling constant $g = \rho_0 J$. To better understand the origin of these states, we introduce a simplified zero-bandwidth model where each screening channel is represented by a single orbital f_i with pairing $(\Delta\, f^\dagger_{i\uparrow} f^\dagger_{i\downarrow} + \text{H.c.})$, and $2\mathbf{s}_i = \sum_{\alpha\beta} f^\dagger_{i\alpha}\, \boldsymbol{\sigma}_{\alpha\beta}\, f_{i\beta}$. The lowest four eigenstates, shown in Fig. 1(b), are in qualitative correspondence with those of the full model. The even-parity $S = 1/2$ state represents a decoupled impurity spin. (The parity refers to the channel inversion symmetry.) This is the GS for low g and corresponds to the local-moment phase at $\Delta > T_K$. Each spin-singlet state corresponds to the impurity spin coupled into an $S = 0$ state to a singly occupied orbital, the other orbital being instead in the configuration $(|0\rangle - |\uparrow\downarrow\rangle)/\sqrt{2}$. There are evidently two such spin-singlet states, depending on which orbital screens the impurity. This is actually the doubly degenerate GS for intermediate values of g. Finally, in the large-g limit the GS is an odd-parity strong-coupling state: both orbitals are singly occupied and coupled into an odd-parity spin-triplet configuration, which is in turn coupled to the impurity into an $S = 1/2$ state.

The low-g and high-g limits are related through a duality mapping that interchanges the parity of the $S = 1/2$ states, and which also occurs in the $\Delta = 0$ model [60,63]. At $g = g^* \approx 0.7$, these states cross and thereby define the self-dual point. This occurs at a particular value of the excitation energy ϵ^* defined in Eq. (1). This value is actually universal: for any g, the two doublet levels converge in the $\Delta \to 0$ limit toward the same value ϵ^*; see Fig. 1(c). In Fig. 2, we plot the subgap $S = 1/2$ states as a function of the dimensionless exchange coupling constant $g = \rho_0 J$ for a range of values for the gap Δ. All curves cross in the self-dual point at $g^* \approx 0.7$. For values of J close to the self-dual point, where the Kondo temperature is of a magnitude comparable to the bandwidth, the universal limit is reached already at high values of Δ.

The self-dual point thus defines the universal nontrivial fixed point of the theory in the small-gap limit, as well as at $\Delta = 0$. The approach toward this limit is a square-root

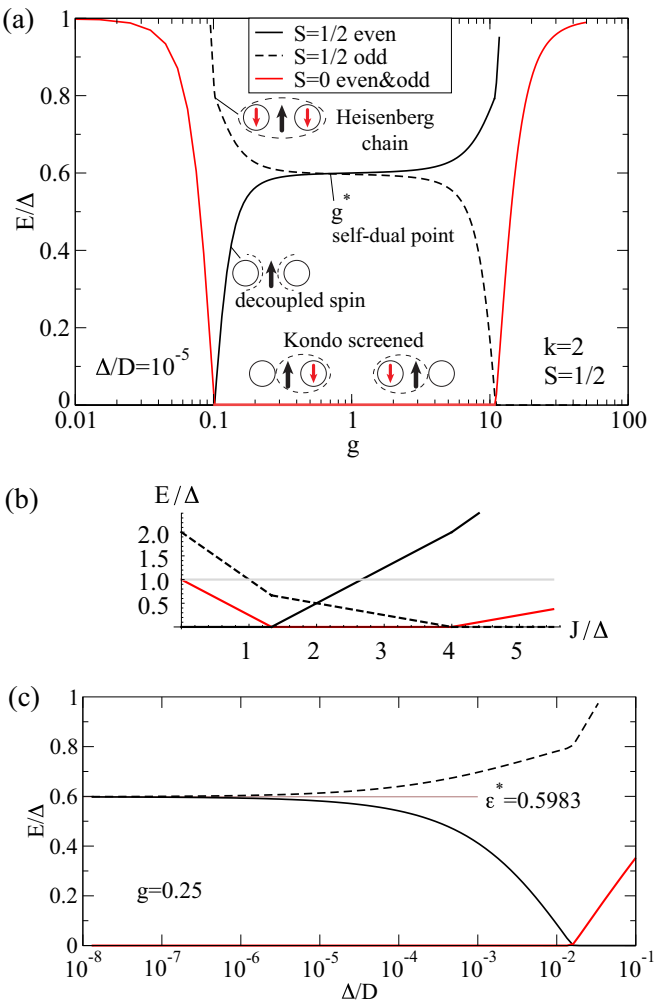

FIG. 1. (a) Subgap many-particle states in the two-channel Kondo (2CK) model with a fixed gap as a function of $g = \rho_0 J$. The energies are given with respect to the ground-state energy. S is the total spin quantum number of the many-particle state. The parity of states (even and odd) refers to the channel inversion symmetry (channel $k = 1$ maps into channel $k = 2$ and vice versa). There are two spin-singlet "Kondo-screened" states where the spin forms a Kondo cloud predominantly with one of the two channels and is essentially decoupled from the other. There are two different spin-doublet states: one where the impurity is decoupled from the channels, and another where it strongly couples to the neighboring orbitals from the two channels to form a three-site antiferromagnetic Heisenberg spin chain. The point where these two states have equal excitation energy defines the self-dual point at $g = g^*$. (b) Eigenstates in the zero-bandwidth limit. (c) Approach toward the asymptotic universal spectrum in the zero-gap limit: as $\Delta \to 0$, the doublet states do not merge with the continuum as in Fermi-liquid systems, but they converge to a finite E/Δ value that is characteristic of the non-Fermi-liquid fixed point.

function of Δ:

$$E_{o,e}/\Delta \sim \epsilon^* + c_{o,e}(g)\Delta^{1/2}. \tag{3}$$

Magnetic anisotropy $J_\perp \neq J_z$ is irrelevant, as in the normal state, and it does not affect the value of ϵ^*. We have also verified that the presence or absence of the particle-hole symmetry plays no role.

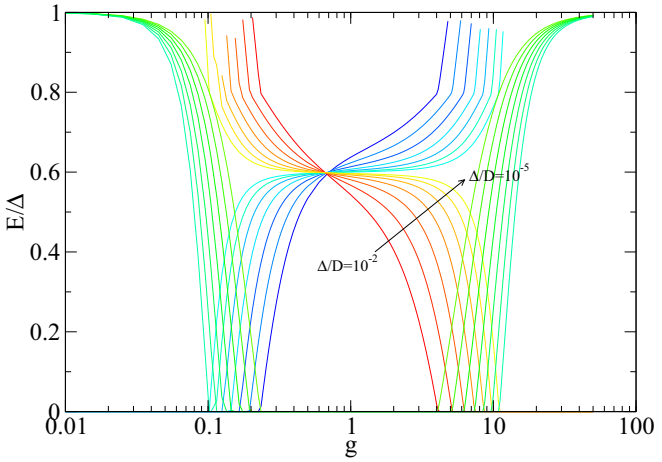

FIG. 2. Subgap $S = 1/2$ many-particle states in the 2CK model for a range of Δ forming a geometric sequence with ratio $\sqrt{10}$.

In Fig. 3 we show the finite-size excitation spectrum (NRG flow diagram) as a function of the Wilson chain length N, corresponding to the energy scale $\varepsilon_N = \Lambda^{-N/2}$. Specifically, Fig. 3(a) reports the energies scaled as $\epsilon = E/\varepsilon_N$, and it demonstrates the crossover from the local moment to the 2CK NFL fixed point for $N \gtrsim 30$, with characteristic fractional energies $\epsilon_N = 0,1/8,1/2,5/8,1,\ldots$ and degeneracies $2,4,10,12,26,\ldots$, respectively, that reflect the peculiar $SU(2)_2 \times SO(5)$ conformal field theory (CFT) that describes the asymptotic behavior of the model at $\Delta = 0$ [41,46,55]. We observe that a finite Δ lowers the SO(5) symmetry down to $SU(2) \times U(1)$, which corresponds to an $SU(2)_2$ CFT times the Z_2 orbifold of a compactified $c = 1$ CFT. The latter allows for a marginal boundary operator that can split the SO(5) multiplets, for instance the degeneracy 4 of the 1/8 state into $4 \to 2+2$, or the degeneracy 10 of the 1/2 state into $10 \to 2+6+2$ (see Sec. VI). Such splitting is already evident in Fig. 3(a) for $40 \lesssim N \lesssim 45$. However, for $N \gtrsim 45$, the BCS gap exceeds ε_N and induces flow toward a new fixed point, which is better characterized by scaling the energies as E/Δ; see Fig. 3(b). The lowest doublet of the split $\epsilon = 1/8$ multiplet becomes the doubly degenerate spin-singlet GS, while the $\epsilon = 0$, $S = 1/2$ state and the lowest $S = 1/2$ state of the split $\epsilon = 1/2$ multiplet meet in the $S = 1/2$ subgap doublet. The continuum of excitations for $E > \Delta$, which is dense close to the gap edge, is best shown scaled as $(E-\Delta)/\Lambda^{-N}$; Fig. 3(c). The energies are spaced by the ratio of Λ, rather than Λ^2 as in the gapped single-channel FL case [23]. Such a progression results from a combination of FL states with one channel having $\delta = 0$ and the other $\delta = \pi/2$ quasiparticle phase shift, as expected for a GS where the Kondo effect is formed with one channel, the other being decoupled. This does not imply, however, that FL behavior is recovered. The degeneracy of states above the gap is twice the number for a FL. More remarkably, when the matrix elements are evaluated to compute the impurity DOS, there are no coherence peaks in the $\Delta \ll T_K$ limit (see Sec. V).

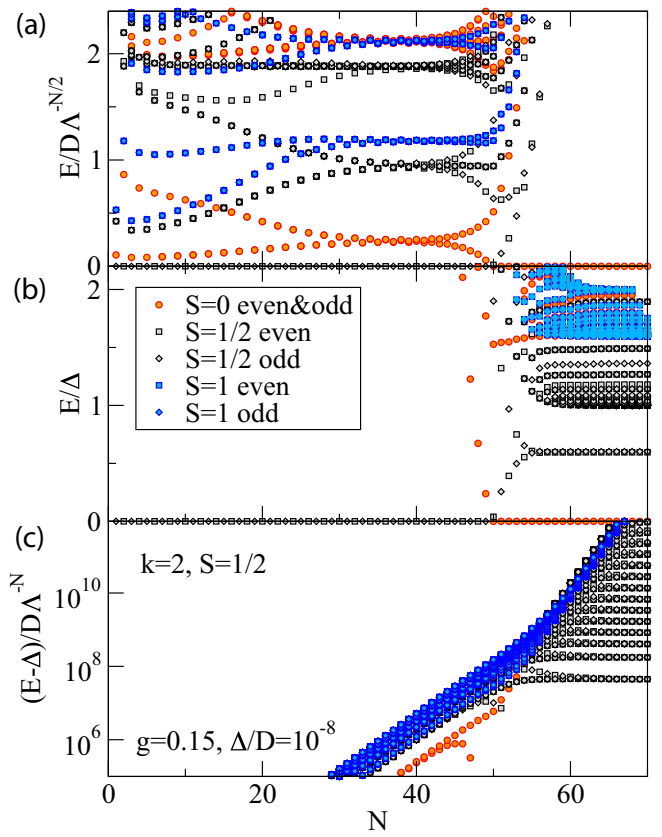

FIG. 3. Renormalization flow diagram with different scalings of the energy axis for the 2CK model. N is the iteration number and $\Lambda = 2$ is the NRG discretization parameter.

B. Three-channel Kondo model

We now turn to the three-channel Kondo (3CK) models with $k = 3$, which also have NFL ground states for $2S < k$ [64–67]. The three-channel Kondo models with $S = 1/2$ and 1 exhibit cross-duality: the small-g limit of the $S = 1/2$ model corresponds to the large-g limit of the $S = 1$ model, and vice versa. This occurs because the overscreening of a spin-1/2 by three channels produces a spin-1 residual object, while overscreening of a spin-1 produces a spin-1/2 residual object. Accordingly, the two models share essentially the same intermediate-coupling NFL fixed point, only shifted by one Wilson shell, i.e., the even and odd system sizes are interchanged; for $S = 1/2$, the level progression is $0,1/8,2/8,5/8,6/8,7/8,\ldots$ with degeneracies $3,12,14,28,42,24$ for odd lengths and $0,2/8,6/8,10/8,\ldots$ with degeneracies $2,6,46,90,\ldots$ for even lengths (for both small and large g), and vice versa for the $S = 1$ model. The Kondo temperature peaks for $g \sim 1$. For finite Δ, the even-odd alternation no longer occurs, and the cross-duality becomes more obvious. For $g \sim 1$, the spin-singlet ground state is triply degenerate, and there are two spin-doublet energy levels, one nondegenerate and one triply degenerate, again with *universal energy ratios*:

$$\epsilon_1^* \equiv E_1^*/\Delta \approx 0.19, \quad \epsilon_3^* \equiv E_3^*/\Delta \approx 0.72. \tag{4}$$

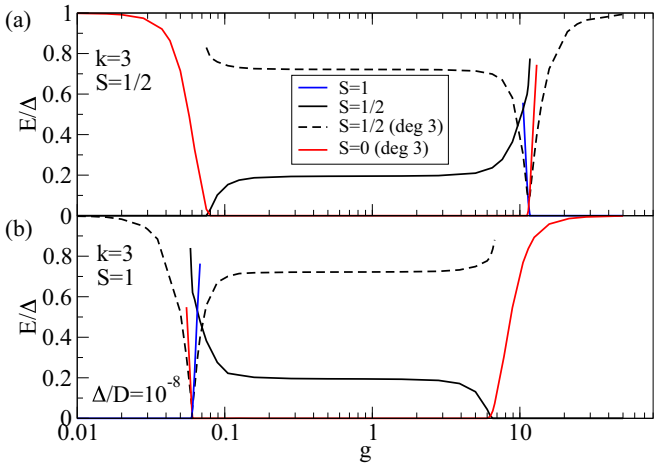

FIG. 4. Subgap many-particle states in the three-channel Kondo (3CK) models with (a) $S = 1/2$ and (b) $S = 1$. Here $\Lambda = 5$.

A spin-triplet subgap state is also present and becomes the ground state in the small-g limit of the $S = 1$ model and in the large-g limit of the $S = 1/2$ model.

The subgap states can be interpreted in the zero-bandwidth limit. For the $S = 1/2$ case, the following holds:

(i) The three spin-singlet states correspond to the Kondo states formed between the impurity spin and one of the three channels, the other two remaining decoupled.

(ii) The nondegenerate spin-doublet 1 is the local-moment state.

(iii) The triply degenerate spin-doublet 3 is composed of spin-1/2 "Heisenberg-chain" states formed between the impurity spin and two of the neighboring orbitals, the third channel being decoupled.

(iv) The spin-triplet is a "Heisenberg-star" state formed by the impurity and all three orbitals.

For the $S = 1$ case, we find the following:

(a) The three spin-singlet states correspond to the exactly screened Kondo states formed between the impurity spin and two of the three channels, the third one remaining decoupled.

(b) The nondegenerate spin-doublet 1 is a "Heisenberg-star" state formed between the impurity spin and the three neighboring orbitals.

(c) The triply degenerate spin-doublets 3 can be thought of as underscreened Kondo states where the impurity spin binds to one of the neighboring orbitals, the other two channels remaining decoupled.

(d) The spin-triplet is the local-moment state.

Because of the duality, the subgap spectra shown in Fig. 4 are essentially mirror images of each other. The nontrivial regime corresponds to the flat parts for intermediate-coupling $g^* \sim 1$. For any g, the $\Delta \to 0$ fixed point is the same. The approach is now

$$E_{1,3}/\Delta \sim \epsilon^*_{1,3} + c_{1,3}\Delta^{1/3}. \tag{5}$$

Compared to the 2CK case, the two subgap states now approach two different values, and the exponent is 1/3 rather than 1/2.

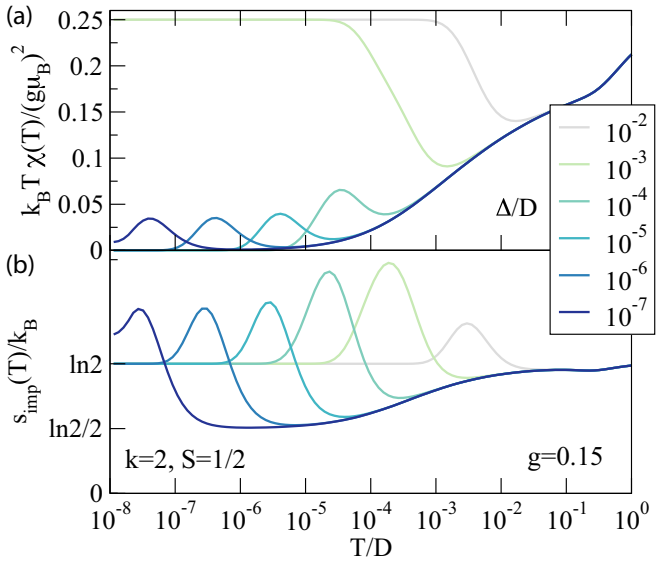

FIG. 5. Temperature dependence of (a) impurity magnetic susceptibility and (b) impurity entropy in the 2CK model.

IV. ANOMALOUS THERMODYNAMICS

The reshuffling of states when the gap opens leads to peculiar thermodynamics. In Fig. 5, we plot the impurity magnetic susceptibility, $\chi_{\rm imp}$, and impurity (boundary) entropy $s_{\rm imp}$ for the two-channel Kondo model. For $T \gg \Delta$, the temperature dependence equals that of the $\Delta = 0$ model: the effective local moment goes to zero and the impurity entropy reaches the $\ln 2/2$ plateau. At $T \sim \Delta$, the effective degeneracy of the impurity-generated states *increases*, leading to peaks in both $\chi_{\rm imp}$ and $s_{\rm imp}$. The boundary entropy thus increases from $\sim \ln 2/2$ to $\ln 2$. The g theorem [68] does not hold here because Δ breaks the conformal invariance. Rising impurity entropy at low temperatures is also found in other related impurity models [69–71].

V. ABSENCE OF COHERENCE PEAKS

The FL properties are restored when the channel symmetry in the overscreened Kondo models is broken [38,56,60–62,72]. The subgap spectrum, shown in Fig. 6(a) as a function of $\Delta J = (J_1 - J_2)/2$ for constant $J_{\rm avg}$ such that $T_K \gg \Delta$, now depends on the relative value of Δ and the NFL-FL crossover scale T^*. For small ΔJ such that $T^* \ll \Delta$, the subgap spectrum is "NFL-like" with the $S = 1/2$ doublet close to ϵ^*. As ΔJ increases, the degeneracy between the spin-singlet states is lifted. The Kondo state in the dominant channel remains the GS, while the other Kondo state rapidly rises in energy and enters the continuum. The subgap $S = 1/2$ doublet asymptotically approaches the gap edge in the large-ΔJ limit, where $T^* \gg \Delta$, and the spectrum becomes "FL-like" with no subgap states (because $\Delta \ll T_K$). The NFL-FL crossover has a characteristic signature also in the impurity DOS; see Fig. 6(b): with increasing ΔJ, the δ peaks move toward the continuum edges, and the spectral weight is transferred from the subgap region into the continuum to form the coherence peaks characteristic of the FL regime.

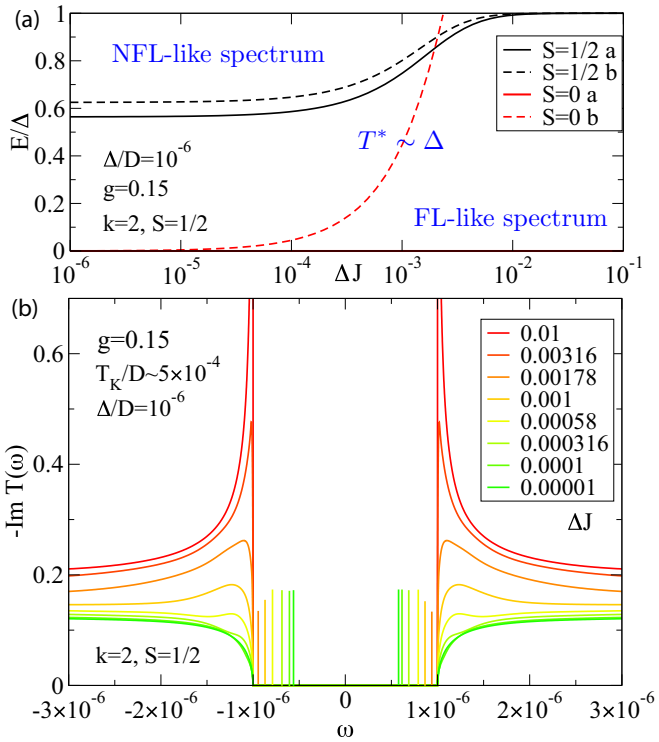

FIG. 6. Channel symmetry breaking, $J_1 \neq J_2$, in the 2CK model. (a) Evolution of the subgap states vs ΔJ; the crossover point $T^* \sim \Delta$ occurs for $\Delta J \approx 10^{-3}$. (b) Impurity spectral function (Im part of the T matrix) for a range of ΔJ.

VI. CFT APPROACH TO THE 2CK

In this section, we will briefly sketch how the conformal field theory (CFT) can be applied to the two-channel Kondo (2CK) model. We will make great use throughout of the results in the book by Di Francesco, Mathieu, and Sénéchal [73]. We will not pretend to be as rigorous and as detailed as they are, we will just limit ourselves to listing some results whose derivation can be obtained relatively easily through that book. Therefore, in this section we implicitly assume that the reader is somewhat familiar with the CFT.

First of all, we assume that the low-energy physics of the model can be reproduced equally well by a simple tight-binding model on a semi-infinite chain, with the impurity spin sitting at the edge. The Hamiltonian thus reads

$$H = -t \sum_{x\geqslant 1} \sum_{a=1}^{2} \sum_{\sigma} (c^\dagger_{x\,a\sigma} c_{x+1\,a\sigma} + c^\dagger_{x+1\,a\sigma} c_{x\,a\sigma}) - \Delta \sum_{x\geqslant 1} \sum_{a=1}^{2} (c^\dagger_{x\,a\uparrow} c^\dagger_{x\,a\downarrow} + c_{x\,a\downarrow} c_{x\,a\uparrow}) + J \sum_{a=1}^{2} \sum_{\alpha\beta} \mathbf{S}\cdot c^\dagger_{1\,a\alpha} \mathbf{S}_{\alpha\beta}\, c_{1\,a\beta} \tag{6}$$

$$\equiv H_0(\Delta) + H_{\rm Kondo}. \tag{7}$$

To identify in a simple way the symmetries of the Hamiltonian, it is convenient to perform the unitary transformation

$$c_{x\,a\uparrow} = \frac{1}{\sqrt{2}} (d_{x\,a\uparrow} - (-1)^x\, d^\dagger_{x\,a\downarrow}),$$

$$c_{x\,a\downarrow} = \frac{1}{\sqrt{2}} (d_{x\,a\downarrow} + (-1)^x\, d^\dagger_{x\,a\uparrow}),$$

which leaves $H_{\rm Kondo}$ invariant, while $H(\Delta)$ transforms into a tight-binding Hamiltonian with a staggered on-site potential:

$$H_0(\Delta) \to -t \sum_{x=1}^{2L} \sum_{a=1}^{2} \sum_{\sigma} (d^\dagger_{x\,a\sigma} d_{x+1\,a\sigma} + d^\dagger_{x+1\,a\sigma} d_{x\,a\sigma}) - \Delta \sum_{x=1}^{2L} \sum_{a=1}^{2} \sum_{\sigma} (-1)^x\, d^\dagger_{x\,a\sigma} d_{x\,a\sigma}. \tag{8}$$

In this representation, it becomes evident that the full Hamiltonian $H = H_0(\Delta) + H_{\rm Kondo}$ is invariant under spin SU(2), channel flavor SU(2), and charge U(1).

A transparent way to build the correct CFT for this model is to equate partition functions via the so-called character decomposition. When $J = \Delta = 0$, the model possesses a large symmetry. As pointed out by Maldacena and Ludwig [46], it is convenient to represent the degrees of freedom of the model in terms of eight chiral Majorana fermions, thus through an SO(8) CFT. We start from the partition function of the $H_0(0)$, namely of two spinful channels, which reads

$$Z = \sum_{n_1,n_2=0}^{1} \left(\chi^{(1)}_{n_1}\, \chi^{(1)}_{n_2}\right)_{\rm charge} \left(\chi^{(1)}_{n_1}\, \chi^{(1)}_{n_2}\right)_{\rm spin}, \tag{9}$$

where $\chi^{(k)}_n$ with $n = 0, \ldots, k$ are the characters of the $SU(2)_k$ CFT, where k is the level, and they are related to primary fields $\boldsymbol{\phi}^{(k)}_n$, of spin $S = n/2$ and dimension $S(S+1)/(k+2)$. In Eq. (9) the $SU(2)_1$ primary fields occur. Since an electron brings both spin 1/2 and charge isospin 1/2, the label $n_a = 0, 1$ in each channel is the same in the spin and charge sectors, where $n_a = 0$ is the contribution to Z of states with an even number of electrons in channel $a = 1,2$, and $n_a = 1$ is the contribution to Z of states with an odd electron number. It is known that

$$\chi^{(1)}_0\, \chi^{(1)}_0 = \left(\chi^I_0\right)^4 + \left(\chi^I_{1/2}\right)^4 + 6\left(\chi^I_0\right)^2 \left(\chi^I_{1/2}\right)^2, \tag{10}$$

$$\chi^{(1)}_1\, \chi^{(1)}_1 = 4\left(\chi^I_0\right)^3 \left(\chi^I_{1/2}\right) + 4\left(\chi^I_0\right) \left(\chi^I_{1/2}\right)^3, \tag{11}$$

$$\chi^{(1)}_0\, \chi^{(1)}_1 = 2\left(\chi^I_{1/16}\right)^4, \tag{12}$$

where χ^I_x are the characters of an Ising CFT with primary fields of dimension 0, 1/16 (σ), and 1/2 (ϵ). Substituting Eqs. (10)–(12) in Eq. (9), one can rewrite the original partition function in terms of the characters of eight Ising CFT, i.e., eight Majorana fermions, and as a benefit get immediately the degeneracy of the states of each conformal tower.

However, three of the eight Majorana fermions merge together into the spin operators that are coupled with the impurity, realizing an $SU(2)_2$ CFT. By means of the known results

$$\chi^{(1)}_0\, \chi^{(1)}_0 = \chi^I_0\, \chi^{(2)}_0 + \chi^I_{1/2}\, \chi^{(2)}_2,$$

$$\chi^{(1)}_0\, \chi^{(1)}_1 = \chi^I_{1/16}\, \chi^{(2)}_1,$$

$$\chi^{(1)}_1\, \chi^{(1)}_1 = \chi^I_0\, \chi^{(2)}_2 + \chi^I_{1/2}\, \chi^{(2)}_0,$$

that describe the combination of two $SU(2)_1$ CFTs into an $SU(2)_2$ plus an Ising, we finally obtain the partition function of the $SO(5) \times SU(2)_2$ CFT, where the $SU(2)_2$ refers to the spin degrees of freedom,

$$Z = \left[\left(\chi_0^I\right)^5 + 10\left(\chi_0^I\right)^3\left(\chi_{1/2}^I\right)^2 + 5\left(\chi_0^I\right)\left(\chi_{1/2}^I\right)^4\right]\chi_0^{(2)} + 4\left(\chi_{1/16}^I\right)^5\chi_1^{(2)} + \left[5\left(\chi_0^I\right)^4\left(\chi_{1/2}^I\right) + 10\left(\chi_0^I\right)^2\left(\chi_{1/2}^I\right)^3 + \left(\chi_{1/2}^I\right)^5\right]\chi_2^{(2)},$$

which therefore represents the partition function in terms of a spin $SU(2)_2$ and five Ising CFTs.

Following the fusion hypothesis [41], the NFL fixed point is obtained after fusion with an $SU(2)_2$ primary field of spin-1/2, and it is characterized by the partition function

$$Z_{\rm NFL} = 4\left(\chi_{1/16}^I\right)^5\left(\chi_0^{(2)} + \chi_2^{(2)}\right) + \left(\chi_0^I + \chi_{1/2}^I\right)^5\chi_1^{(2)}. \quad (13)$$

The ground state belongs to the tower $(\chi_0^I)^5\,\chi_1^{(2)}$ with energy $E_0 = 3/16$. The next lying state corresponds to $4\left(\chi_{1/16}^I\right)^5\chi_0^{(2)}$. It is fourfold degenerate, and its energy with respect to the ground state one is $E_{1/8} = 5/16 - 3/16 = 1/8$. Above it there are several states with an energy difference from the ground state of $E_{1/2} = 1/2$. These correspond explicitly to the terms $5(\chi_0^I)^4\left(\chi_{1/2}^I\right)\chi_1^{(2)}$, hence a tenfold degeneracy since $\chi_1^{(2)}$ has spin $S = 1/2$. One can proceed further and obtain all levels and their degeneracies.

When $\Delta \neq 0$, it is more convenient to extract out of the five Majorana fermions those three that combine to produce a flavor $SU(2)_2$. This is readily done by observing that

$$\left(\chi_0^I + \chi_{1/2}^I\right)^5 = \left(\chi_0^I + \chi_{1/2}^I\right)^2\left(\chi_0^{(2)} + \chi_2^{(2)}\right),$$
$$4\left(\chi_{1/16}^I\right)^5 = 2\left(\chi_{1/16}^I\right)^2\chi_1^{(2)},$$

so that we can rewrite Eq. (13) as

$$Z_{\rm NFL} = \mathbf{2}\left(\chi_{1/16}^I\right)^2\left(\chi_1^{(2)}\right)_{\rm flavor}\left(\chi_0^{(2)} + \chi_2^{(2)}\right)_{\rm spin} + \left(\chi_0^{I\,2} + \chi_{1/2}^{I\,2} + \mathbf{2}\,\chi_0^I\,\chi_{1/2}^I\right)\left(\chi_0^{(2)} + \chi_2^{(2)}\right)_{\rm flavor}\left(\chi_1^{(2)}\right)_{\rm spin}. \quad (14)$$

The two Ising CFTs can in turn be recombined in a $c = 1$ CFT on compactification radius $R = \sqrt{2p'} = 2$, which has the following primary fields:

(i) $\phi_{1/8}$ with dimension 1/8.

(ii) A doubly degenerate field $\phi_{1/2}^{(a)}, a = 1,2$, with dimension 1/2.

(iii) The twist operators $\sigma^{(a)}$ and $\tau^{(a)}$ with dimensions 1/16 and 9/16, respectively.

(iv) The dimension 1 operator θ.

It is just the latter operator θ that becomes allowed at the boundary and which lifts the degeneracy indicated in Eq. (14) by a bold **2**. In Table I we tabulate the NRG finite-size spectrum at $\Lambda = 2$ in the presence of a small local Δ term on the first site of the chain.

TABLE I. Energy levels of the two-channel Kondo (2CK) model upon including a local Δ term on the first site of the Wilson chain. The small deviation from exact values in the progression $0, 1/8, 1/2, 5/8, \ldots$ at $\Delta = 0$ is a discretization effect.

Q	S	P	deg	$\epsilon(0)$	$\epsilon(\Delta)$
0	1/2	even	2	0	0
–1	0	even,odd	2	0.125	0.1206
1	0	even,odd	2	0.125	0.1290
–2	1/2	odd	2	0.498	0.4897
0	1/2	2 × odd,even	6	0.498	0.4980
2	1/2	odd	2	0.498	0.5063
–1	1	even,odd	6	0.621	0.6165
1	1	even,odd	6	0.621	0.6247

VII. ANDERSON-YUVAL APPROACH IN THE PRESENCE OF A STAGGERED POTENTIAL

We now sketch an analytical argument that explains qualitatively and to some extent also quantitatively the NRG results for the two-channel Kondo model in the presence of the superconducting gap. We consider the model defined by Eq. (8), i.e., a tight-binding model in the presence of a staggered potential Δ, and we apply a simplified version of the Anderson-Yuval approach to the Kondo effect [74–76]. The unperturbed spectrum is $\pm E_k = \pm\sqrt{\epsilon_k^2 + \Delta^2}$, and we shall assume a constant DOS ρ for $\epsilon_k \in [-D, D]$ with $D \gg \Delta$. The first step is to consider the scattering problem for a frozen impurity (no spin-flip term). Supposing the impurity spin is down, then the spin-up electrons will feel an attractive potential, $-J_z/4$, whereas the spin-down electrons will feel a repulsive one, $+J_z/4$. We will briefly define the potential V, including both possibilities $V = \pm J_z/4$. The variation of the DOS for a single spin species due to the impurity is

$$\Delta\rho(\epsilon) = -\frac{1}{\pi}\frac{\partial}{\partial\epsilon}\,\mathrm{Arg}\ln(1 - VG(\epsilon)).$$

We define $\Gamma(\epsilon) = 1 - VG(\epsilon)$. $G(z)$ is the unperturbed local Green's function depending on the complex frequency z,

$$G(z) = -2\rho\,(z + \Delta)\int_0^D d\omega\,\frac{1}{\omega^2 - z^2 + \Delta^2},$$

while $G(\epsilon) = G(z = \epsilon + i0^+)$. Hereafter, we take $\Delta > 0$, which actually corresponds to the case in which at the impurity site the staggered potential is $+\Delta > 0$. We find the following:

(i) $\epsilon^2 < \Delta^2$,

$$G(\epsilon) = -2\rho\,\frac{\epsilon + \Delta}{\sqrt{\Delta^2 - \epsilon^2}}\,\tan^{-1}\frac{D}{\sqrt{\Delta^2 - \epsilon^2}} \simeq -\pi\,\rho\,\frac{\epsilon + \Delta}{\sqrt{\Delta^2 - \epsilon^2}}.$$

In the second line, we took the $D \to \infty$ limit. In this case,

$$\Gamma(\epsilon) = 1 + \pi\,\rho\,V\sqrt{\frac{\Delta + \epsilon}{\Delta - \epsilon}}.$$

If $V > 0$, then $\Gamma(\epsilon) > 0\,\forall\,\epsilon \in [-\Delta, \Delta]$. If $V < 0$, then $\Gamma(\epsilon) > 0$ for $\epsilon \in [-\Delta, \epsilon_*]$, it changes sign at ϵ_*, and $\Gamma(\epsilon) < 0$ for

$\epsilon \in [\epsilon_*, \Delta]$. Here

$$\epsilon_* = \Delta \, \frac{1-(\pi\,\rho\,V)^2}{1+(\pi\,\rho\,V)^2}.$$

In the vicinity of ϵ_*, $\Gamma(\epsilon) = -(\epsilon-\epsilon^*)/\Delta$.

The self-dual point is actually identified by [76]

$$\left(\pi\,\rho\,V\right)^2 = 1,$$

so that $\epsilon_* = 0$. It corresponds to a genuine bound state just in the center of the gap.

(ii) $\Delta^2 < \epsilon^2 < D^2 + \Delta^2$,

$$G(\epsilon) = -i\pi\,\rho\,\mathrm{sgn}(\epsilon)\,\frac{\epsilon+\Delta}{\sqrt{\epsilon^2-\Delta^2}} + \rho\,\frac{\epsilon+\Delta}{\sqrt{\epsilon^2-\Delta^2}}\,\ln\frac{D+\sqrt{\epsilon^2-\Delta^2}}{D-\sqrt{\epsilon^2-\Delta^2}}.$$

It follows that

$$\mathrm{Re}\,\Gamma(\epsilon) = 1 - V\rho\,\frac{\epsilon+\Delta}{\sqrt{\epsilon^2-\Delta^2}} \times \ln\frac{D+\sqrt{\epsilon^2-\Delta^2}}{D-\sqrt{\epsilon^2-\Delta^2}},$$

$$\mathrm{Im}\,\Gamma(\epsilon) = \pi\rho V\,\mathrm{sgn}(\epsilon)\,\frac{\epsilon+\Delta}{\sqrt{\epsilon^2-\Delta^2}}.$$

(iii) $\epsilon^2 > D^2 + \Delta^2$,

$$G(\epsilon) = \rho\,\frac{\epsilon+\Delta}{\sqrt{\epsilon^2-\Delta^2}}\,\ln\frac{\sqrt{\epsilon^2-\Delta^2}+D}{\sqrt{\epsilon^2-\Delta^2}-D}.$$

Then $\mathrm{Im}\,\Gamma(\epsilon) = 0$, while

$$\mathrm{Re}\,\Gamma(\epsilon) = 1 - V\,\frac{\epsilon+\Delta}{\sqrt{\epsilon^2-\Delta^2}}\,\ln\frac{\sqrt{\epsilon^2-\Delta^2}+D}{\sqrt{\epsilon^2-\Delta^2}-D}.$$

It follows that, if $D \gg \Delta$ and $\epsilon^2 \ll D^2$,

$$\Gamma(\epsilon) = \begin{cases} 1+\pi\,\rho\,V\sqrt{\dfrac{\Delta+\epsilon}{\Delta-\epsilon}}, & \epsilon^2 < \Delta^2, \\ 1+i\pi\,\rho\,V\,\mathrm{sgn}(\epsilon)\sqrt{\dfrac{\epsilon+\Delta}{\epsilon-\Delta}}, & \Delta^2 < \epsilon^2 \ll D^2. \end{cases}$$

At the self-dual point $\pi\rho V = \mathrm{sgn}(V)$, thus we rewrite the above as

$$\Gamma(\epsilon) = \begin{cases} 1+\mathrm{sgn}(V)\sqrt{\dfrac{\Delta+\epsilon}{\Delta-\epsilon}}, & \epsilon^2 < \Delta^2, \\ 1+i\,\mathrm{sgn}(V)\,\mathrm{sgn}(\epsilon)\sqrt{\dfrac{\epsilon+\Delta}{\epsilon-\Delta}}, & \Delta^2 < \epsilon^2 \ll D^2. \end{cases}$$

The retarded local Green's function reads

$$\mathcal{G}_R(\epsilon) = \frac{G(\epsilon)}{\Gamma(\epsilon)}.$$

In the limit of very large bandwidth so that $\epsilon^2 \ll D^2$, we find for $\epsilon^2 < \Delta^2$

$$\mathcal{G}_R(\epsilon) = -\pi\,\rho\,\frac{\sqrt{\Delta+\epsilon}}{\sqrt{\Delta-\epsilon}+\pi\rho V\sqrt{\Delta+\epsilon}}.$$

For $V < 0$, at the self-dual point with $\epsilon^* = 0$, its DOS has a midgap bound state,

$$\mathcal{A}(\epsilon) = -\frac{1}{\pi}\,\mathrm{Im}\,\mathcal{G}(\epsilon) = \pi\,\rho\,\Delta\,\delta(\epsilon).$$

The scattering phase shift is defined as

$$\delta_V(\epsilon) = \arg[\Gamma(\epsilon)], \tag{15}$$

which implies in this case

$$\tan\delta_V(\epsilon) = \mathrm{sgn}(V)\sqrt{\frac{\epsilon+\Delta}{\epsilon-\Delta}}.$$

Indeed, if $\Delta = 0$ or $\epsilon^2 \gg \Delta^2$, we recover the value at the self-dual point,

$$\delta_V(\epsilon) = \mathrm{sgn}(V)\,\frac{\pi}{4}.$$

On the contrary, if $\epsilon^2 \to \Delta^2$, we find that for $V > 0$,

$$\delta_V(\epsilon \to \Delta) = \frac{\pi}{2}, \qquad \delta_V(\epsilon \to -\Delta) = 0.$$

Indeed, for any $\eta > 0$,

$$\delta_+(\Delta+\eta) = \frac{\pi}{2} - \delta_+(-\Delta-\eta).$$

We now include in the consideration also the transverse exchange

$$H_\perp = \frac{J_\perp}{2}\sum_{a=1,2}\left(S^-\,\Psi^\dagger_{a\uparrow}(0)\,\Psi_{a\downarrow}(0) + \mathrm{H.c.}\right),$$

where

$$\Psi_\sigma(0) = \sum_\epsilon \psi_{\epsilon\sigma}(0)\,c_{\epsilon\sigma},$$

with $\psi_\epsilon(0)$ the amplitude of the eigenfunction of energy ϵ at the impurity site. In particular, at the self-dual point, the bound state $c_{\epsilon=0\sigma} \equiv d_\sigma$ has

$$\psi_0(0) = \sqrt{\rho\,\Delta},$$

so that, if the impurity is down,

$$\Psi_\uparrow(0) = \sqrt{\rho\,\Delta}\;d_\uparrow + \sum_{\epsilon^2>\Delta^2}\psi_{\epsilon\uparrow}(0)\,c_{\epsilon\uparrow},$$

$$\Psi_\downarrow(0) = \sum_{\epsilon^2>\Delta^2}\psi_{\epsilon\downarrow}(0)\,c_{\epsilon\downarrow},$$

while if the impurity is up,

$$\Psi_\uparrow(0) = \sum_{\epsilon^2>\Delta^2}\psi_{\epsilon\downarrow}(0)\,c_{\epsilon\uparrow},$$

$$\Psi_\downarrow(0) = \sqrt{\rho\,\Delta}\;d_\downarrow + \sum_{\epsilon^2>\Delta^2}\psi_{\epsilon\uparrow}(0)\,c_{\epsilon\downarrow}.$$

Suppose we just consider the contribution to the spin-flip of the bound state, namely within the subspace of the four states,

$$|a,\downarrow\rangle = |\downarrow\rangle \times d^\dagger_{a\uparrow}\,|\Phi_\downarrow\rangle,$$

$$|a,\uparrow\rangle = |\uparrow\rangle \times d^\dagger_{a\downarrow}\,|\Phi_\uparrow\rangle,$$

where $|\Phi_\sigma\rangle$ is the Slater determinant where the valence band is fully occupied and the conduction one empty, which depends

on the impurity spin since the single-particle wave functions have different phase shifts. One trivially finds that

$$\langle a,\downarrow|\, H_\perp \,|\, a,\uparrow\rangle = \frac{J_\perp}{2}\,\rho\,\Delta\,\langle\Phi_\downarrow \mid \Phi_\uparrow\rangle,$$

where the overlap

$$\langle\Phi_\downarrow \mid \Phi_\uparrow\rangle \sim \exp\left[-\frac{8}{\pi^2}\int_{-D}^{-\Delta} d\epsilon\, d\epsilon'\,\frac{\delta(\epsilon)\,\delta(\epsilon')}{(\epsilon+\epsilon')^2}\right] \simeq \sqrt{\frac{\Delta}{D}},$$

which does not vanish despite the orthogonality catastrophe because the gap cuts off the singularity. Therefore, the antisymmetric combination of the two states, which is a spin singlet but doubly degenerate since the bound state is occupied in one channel but empty in the other, has energy lower by $\Delta E \sim J_\perp(\Delta\rho)^{3/2}$ than the states where the bound state is occupied in each channel or when they are not occupied at all, both states being actually degenerate. Evidently, this is just the first order in perturbation theory. One needs higher-order terms. In the spirit of Ref. [75], see also Ref. [44], the spin flip grows by integrating out the high-energy degrees of freedom and asymptotically its dimension lowers to $1/2$. However, in the presence of a gap, one cannot push the renormalization down to zero frequency but must stop at an energy of the order of Δ. We thus expect that the net effect is an upward renormalization of $J_\perp$:

$$J_\perp \to J_{\perp *} \sim \frac{J_\perp}{\sqrt{\rho\,\Delta}},$$

so that the energy of the aforementioned doubly degenerate singlet changes into

$$\Delta E_* \sim -\frac{J_\perp}{2}\,\rho\,\Delta,$$

followed by the $S=1/2$ states in which each channel has the bound state either empty or occupied, at energy 0, and by the doubly degenerate triplet at energy $-\Delta E_*$. If the model is spin-isotropic, $J_\perp = J_z = J$, and the Kondo exchange is at the dual point,

$$\pi\,\rho\,\frac{J}{4} = 1,$$

then

$$\Delta E_* \simeq -\frac{2}{\pi}\,\Delta \simeq -0.636\,62\,\Delta.$$

In other words, within such a very rough approximation, the ground state is indeed the even/odd spin singlet with charge $Q=1$, followed at energy $\simeq 0.636\,62\,\Delta$ by two $S=1/2$ states with charge $Q=0$ or 2. Above energy Δ the continuum starts.

TABLE II. Quantum numbers and the energies of the lowest-lying many-particle states in the two-channel Kondo model with $g=0.25$ and $\Delta/D = 10^{-6}$.

Q	S	P	E/Δ
1	0	odd	0
1	0	even	0
2	1/2	even	0.59
0	1/2	odd	0.60

The subgap many-particle states computed with the NRG for the 2CK with $g=0.25$ and $\Delta/D = 10^{-6}$ are tabulated in Table II.

VIII. CONCLUSION

We speculate that impurity models with Kondo overscreening generically flow in the small-gap limit to fixed points with characteristic persistent bound states of NFL character. More generally, let us imagine adding the mass term Δ first at the impurity site. This term does not correspond to any of the relevant boundary operators at the NFL fixed point, nevertheless it lowers the symmetry and allows for a marginal boundary operator. If this is the case, we argue that an arbitrarily weak mass term of that kind added at the impurity site as well as in the bulk will induce subgap states with universal ratios.

The predicted universal spectra could be tested in experimental setups involving semiconductor nanowire quantum dots coupled to superconducting electrodes. Such setups have been refined in recent years due to the search for Majorana zero modes, which are predicted to occur in such systems. One possibility would be building a mesoscopic superconducting island serving the same role as the "metallic grain" in the setup in Refs. [35,36]. Alternatively, a Majorana box contacted by superconducting leads maps to the same model and should hence host the same universal excitations [77].

ACKNOWLEDGMENTS

R.Ž. acknowledges the support of the Slovenian Research Agency (ARRS) under P1-0044 and J1-7259, and a discussion with A. K. Mitchell. M.F. was party supported by the EU Project No. 692670–FIRSTORM.

[1] P. W. Anderson, Theory of dirty superconductors, J. Phys. Chem. Solids **11**, 26 (1959).
[2] L. Yu, Bound state in superconductors with paramagnetic impurities, Acta Phys. Sin. **21**, 75 (1965).
[3] H. Shiba, Classical spins in superconductors, Prog. Theor. Phys. **40**, 435 (1968).
[4] A. I. Rusinov, Superconductivity near a paramagnetic impurity, Zh. Eksp. Teor. Fiz. Pis'ma Red. **9**, 146 (1968) [JETP Lett. **9**, 85 (1969)].
[5] A. Sakurai, Comments on superconductors with magnetic impurities, Prog. Theor. Phys. **44**, 1472 (1970).
[6] J. Zittartz and E. Müller-Hartmann, Green's function theory of the Kondo effect in dilute magnetic alloys, Z. Phys. **212**, 380 (1968).
[7] R. Žitko, O. Bodensiek, and Th. Pruschke, Magnetic anisotropy effects on quantum impurities in superconducting host, Phys. Rev. B **83**, 054512 (2011).
[8] C. P. Moca, E. Demler, B. Jankó, and G. Zaránd, Spin-resolved

spectra of Shiba multiplets from Mn impurities in MgB_2, Phys. Rev. B **77**, 174516 (2008).

[9] A. V. Balatsky, I. Vekhter, and J.-X. Zhu, Impurity-induced states in conventional and unconventional superconductors, Rev. Mod. Phys. **78**, 373 (2006).

[10] J.-D. Pillet, C. H. L. Quay, P. Morin, C. Bena, A. Levy Yeyati, and P. Joyez, Andreev bound states in supercurrent-carrying carbon nanotubes revealed, Nat. Phys. **6**, 965 (2010).

[11] R. S. Deacon, Y. Tanaka, A. Oiwa, R. Sakano, K. Yoshida, K. Shibata, K. Hirakawa, and S. Tarucha, Tunneling Spectroscopy of Andreev Energy Levels in a Quantum Dot Coupled to a Superconductor, Phys. Rev. Lett. **104**, 076805 (2010).

[12] R. Maurand, T. Meng, E. Bonet, S. Florens, L. Marty, and W. Wernsdorfer, First-Order 0-π Quantum Phase Transition in the Kondo Regime of a Superconducting Carbon-Nanotube Quantum Dot, Phys. Rev. X **2**, 011009 (2012).

[13] S. H. Ji, T. Zhang, Y. S. Fu, X. Chen, X.-C. Ma, J. Li, W.-H. Duan, J.-F. Jia, and Q.-K. Xue, High-Resolution Scanning Tunneling Spectroscopy of Magnetic Impurity Induced Bound States in the Superconducting Gap of Pb Thin Films, Phys. Rev. Lett. **100**, 226801 (2008).

[14] K. J. Franke, G. Schulze, and J. I. Pascual, Competition of superconductivity phenomena and Kondo screening at the nanoscale, Science **332**, 940 (2011).

[15] N. Hatter, B. W. Heinrich, M. Ruby, J. I. Pascual, and K. J. Franke, Magnetic anisotropy in Shiba bound states across a quantum phase transition, Nat. Commun. **6**, 8988 (2016).

[16] K. Satori, H. Shiba, O. Sakai, and Y. Shimizu, Numerical renormalization group study of magnetic impurities in superconductors, J. Phys. Soc. Jpn. **61**, 3239 (1992).

[17] O. Sakai, Y. Shimizu, H. Shiba, and K. Satori, Numerical renormalization group study of magnetic impurities in superconductors. II. Dynamical excitations spectra and spatial variation of the order parameter, J. Phys. Soc. Jpn. **62**, 3181 (1993).

[18] T. Yoshioka and Y. Ohashi, Ground state properties and localized excited states around a magnetic impurity described by the anisotropic *s-d* interaction in superconductivity, J. Phys. Soc. Jpn. **67**, 1332 (1998).

[19] T. Yoshioka and Y. Ohashi, Numerical renormalization group studies on single impurity Anderson model in superconductivity: A unified treatment of magnetic, nonmagnetic impurities, and resonance scattering, J. Phys. Soc. Jpn. **69**, 1812 (2000).

[20] M.-S. Choi, M. Lee, K. Kang, and W. Belzig, Kondo effect and Josephson current through a quantum dot between two superconductors, Phys. Rev. B **70**, 020502 (2004).

[21] A. Oguri, Y. Tanaka, and A. C. Hewson, Quantum phase transition in a minimal model for the Kondo effect in a Josephson junction, J. Phys. Soc. Jpn. **73**, 2494 (2004).

[22] J. Bauer, A. Oguri, and A. C. Hewson, Spectral properties of locally correlated electrons in a Bardeen-Cooper-Schrieffer superconductor, J. Phys.: Condens. Matter **19**, 486211 (2007).

[23] T. Hecht, A. Weichselbaum, J. von Delft, and R. Bulla, Numerical renormalization group calculation of near-gap peaks in spectral functions of the Anderson model with superconducting leads, J. Phys. Condens. Matter **20**, 275213 (2008).

[24] P. Nozières, A "fermi-liquid" description of the Kondo problem at low temperatures, J. Low. Temp. Phys. **17**, 31 (1974).

[25] A. C. Hewson, *The Kondo Problem to Heavy-Fermions* (Cambridge University Press, Cambridge, 1993).

[26] W. Koller, A. C. Hewson, and D. Meyer, Singular dynamics of underscreened magnetic impurity models, Phys. Rev. B **72**, 045117 (2005).

[27] P. Mehta, N. Andrei, P. Coleman, L. Borda, and G. Zaránd, Regular and singular Fermi-liquid fixed points in quantum impurity models, Phys. Rev. B **72**, 014430 (2005).

[28] D. C. Mattis, Symmetry of Ground State in a Dilute Magnetic Metal Alloy, Phys. Rev. Lett. **19**, 1478 (1968).

[29] P. Nozières and A. Blandin, Kondo effect in real metals, J. Phys. (Paris) **41**, 193 (1980).

[30] D. M. Cragg and P. Lloyd, Kondo Hamiltonians with a non-zero ground-state spins, J. Phys. C **12**, L215 (1979).

[31] D. M. Cragg, P. Lloyd, and P. Nozières, On the ground states of some s-d exchange Kondo Hamiltonians, J. Phys. C **13**, 803 (1980).

[32] V. T. Rajan, J. H. Lowenstein, and N. Andrei, Thermodynamics of the Kondo Model, Phys. Rev. Lett. **49**, 497 (1982).

[33] P. D. Sacramento and P. Schlottmann, Thermodynamics of the single-channel Kondo impurity of spin $S(\leqslant 7/2)$ in a magnetic field, Phys. Rev. B **40**, 431 (1989).

[34] Y. Oreg and D. Goldhaber-Gordon, Two-Channel Kondo Effect in a Modified Single Electron Transistor, Phys. Rev. Lett. **90**, 136602 (2003).

[35] R. M. Potok, I. G. Rau, H. Shtrikman, Y. Oreg, and D. Goldhaber-Gordon, Observation of the two-channel Kondo effect, Nature (London) **446**, 167 (2007).

[36] A. J. Keller, L. Peeters, C. P. Moca, I. Weymann, D. Mahalu, V. Umansky, G. Zaránd, and D. Goldhaber-Gordon, Universal Fermi liquid crossover and quantum criticality in a mesoscopic system, Nature (London) **526**, 237 (2015).

[37] Z. Iftikhar, S. Jezouin, A. Anthore, U. Gennser, F. D. Parmentier, A. Cavanna, and F. Pierre, Two-channel Kondo effect and renormalization flow with macroscopic quantum charge states, Nature (London) **526**, 233 (2015).

[38] A. K. Mitchell, L. A. Landau, L. Fritz, and E. Sela, Universality and Scaling in a Charge Two-Channel Kondo Device, Phys. Rev. Lett. **116**, 157202 (2016).

[39] L. J. Zhu, S. H. Nie, P. Xiong, P. Schlottmann, and J. H. Zhao, Orbital two-channel Kondo effect in epitaxial ferromagnetic $L1_0$-MnAl films, Nat. Commun. **7**, 10817 (2016).

[40] I. Affleck, Non-Fermi liquid behavior in Kondo models, J. Phys. Soc. Jpn. **74**, 59 (2005).

[41] I. Affleck and A. W. W. Ludwig, Critical theory of overscreened Kondo fixed points, Nucl. Phys. B **360**, 641 (1991).

[42] I. Affleck and A. W. W. Ludwig, The Kondo effect, conformal field theory and fusion rules, Nucl. Phys. B **352**, 849 (1991).

[43] A. W. W. Ludwig and I. Affleck, Exact, Asymptotic, Three-Dimensional, Space- and Time-Dependent, Green's Functions in the Multichannel Kondo Effect, Phys. Rev. Lett. **67**, 3160 (1991).

[44] V. J. Emery and S. Kivelson, Mapping of the two-channel Kondo problem to a resonant-level model, Phys. Rev. B **46**, 10812 (1992).

[45] P. Coleman, L. B. Ioffe, and A. M. Tsvelik, Simple formulation of the two-channel Kondo model, Phys. Rev. B **52**, 6611 (1995).

[46] J. M. Maldacena and A. W. W. Ludwig, Majorana fermions, exact mapping between quantum impurity fixed points with four

bulk fermion species, and solution of the "unitarity puzzle", Nucl. Phys. B **506**, 565 (1997).
[47] N. Andrei and C. Destri, Solution of the Multichannel Kondo Problem, Phys. Rev. Lett. **52**, 364 (1984).
[48] P. B. Wiegmann and A. M. Tsvelik, Solution of the Kondo problem for an orbital singlet, JETP Lett. **38**, 591 (1983).
[49] P. Schlottmann and P. D. Sacramento, Multichannel Kondo problem and some applications, Adv. Phys. **42**, 641 (1993).
[50] K. G. Wilson, The renormalization group: Critical phenomena and the Kondo problem, Rev. Mod. Phys. **47**, 773 (1975).
[51] H. R. Krishna-murthy, J. W. Wilkins, and K. G. Wilson, Renormalization-group approach to the Anderson model of dilute magnetic alloys. I. Static properties for the symmetric case, Phys. Rev. B **21**, 1003 (1980).
[52] R. Bulla, T. Costi, and T. Pruschke, The numerical renormalization group method for quantum impurity systems, Rev. Mod. Phys. **80**, 395 (2008).
[53] R. Žitko and T. Pruschke, Energy resolution and discretization artefacts in the numerical renormalization group, Phys. Rev. B **79**, 085106 (2009).
[54] R. Žitko, Adaptive logarithmic discretization for numerical renormalization group methods, Comput. Phys. Commun. **180**, 1271 (2009).
[55] D. L. Cox and A. Zawadowski, Exotic Kondo effects in metals: Magnetic ions in a crystalline electric field and tunneling centres, Adv. Phys. **47**, 599 (1998).
[56] I. Affleck, A. W. W. Ludwig, H.-B. Pang, and D. L. Cox, Relevance of anisotropy in the multichannel Kondo effect: Comparison of conformal field theory and numerical renormalization-group results, Phys. Rev. B **45**, 7918 (1992).
[57] I. Affleck and A. W. W. Ludwig, Exact conformal-field-theory results on the multichannel Kondo effect: Single-fermion Green's function, self-energy, and resistivity, Phys. Rev. B **48**, 7297 (1993).
[58] J. von Delft, G. Zaránd, and M. Fabrizio, Finite-Size Bosonization of 2-Channel Kondo Model: A Bridge Between Numerical Renormalization Group and Conformal Field Theory, Phys. Rev. Lett. **81**, 196 (1998).
[59] G. Zaránd and J. von Delft, Analytical calculation of the finite-size crossover spectrum of the anisotropic two-channel Kondo model, Phys. Rev. B **61**, 6918 (2000).
[60] H. B. Pang and D. L. Cox, Stability of the fixed point of the two-channel Kondo Hamiltonian, Phys. Rev. B **44**, 9454 (1991).
[61] E. Sela, A. K. Mitchell, and L. Fritz, Exact Crossover Green Function in the Two-Channel and Two-Impurity Kondo Models, Phys. Rev. Lett. **106**, 147202 (2011).
[62] A. K. Mitchell and E. Sela, Universal low-temperature crossover in two-channel Kondo models, Phys. Rev. B **85**, 235127 (2012).
[63] C. Kolf and J. Kroha, Strong versus weak coupling duality and coupling dependence of the Kondo temperature in the two-channel Kondo model, Phys. Rev. B **75**, 045129 (2007).
[64] Lorenzo de Leo, Non-Fermi liquid behavior in multi-orbital Anderson impurity models and possible relevance for strongly correlated lattice models, Ph.D. thesis, SISSA, Trieste, 2004.
[65] L. De Leo and M. Fabrizio, Surprises in the Phase Diagram of an Anderson Impurity Model for a Single C_{60}^{n-} Molecule, Phys. Rev. Lett. **94**, 236401 (2005).
[66] A. K. Mitchell, M. R. Galpin, S. Wilson-Fletcher, D. E. Logan, and R. Bulla, Generalized Wilson chain for solving multichannel quantum impurity problems, Phys. Rev. B **89**, 121105(R) (2014).
[67] K. M. Stadler, A. K. Mitchell, J. von Delft, and A. Weichselbaum, Interleaved numerical renormalization group as an efficient multiband impurity solver, Phys. Rev. B **93**, 235101 (2016).
[68] I. Affleck and A. W. W. Ludwig, Universal Noninteger Ground-State Degeneracy in Critical Quantum Systems, Phys. Rev. Lett. **67**, 161 (1991).
[69] S. Florens and A. Rosch, Climbing the Entropy Barrier: Driving the Single- Towards the Multichannel Kondo Effect by a Weak Coulomb Blockade of the Leads, Phys. Rev. Lett. **92**, 216601 (2004).
[70] L. Fritz and M. Vojta, Phase transitions in the pseudogap anderson and Kondo models: Critical dimensions, renormalization group, and local-moment criticality, Phys. Rev. B **70**, 214427 (2004).
[71] R. Žitko and T. Pruschke, Anomaly in the heat capacity of Kondo superconductors, Phys. Rev. B **79**, 012507 (2009).
[72] R. Žitko and J. Bonča, Fermi-Liquid Versus Non-Fermi-Liquid Behavior in Triple Quantum Dots, Phys. Rev. Lett. **98**, 047203 (2007).
[73] P. Di Francesco, P. Mathieu, and D. Sénéchal, *Conformal Field Theory* (Springer-Verlag, New York, 1995).
[74] G. Yuval and P. W. Anderson, Exact results for the Kondo problem: One-body theory and extension to finite temperature, Phys. Rev. B **1**, 1522 (1970).
[75] P. W. Anderson, G. Yuval, and D. R. Hamann, Exact results in the Kondo problem. ii. Scaling theory, qualitatively correct solution, and some new results on one-dimensional classical statistical models, Phys. Rev. B **1**, 4464 (1970).
[76] M. Fabrizio, A. O. Gogolin, and P. Nozières, Crossover from Non-Fermi-Liquid to Fermi-Liquid Behavior in the Two Channel Kondo Model with Channel Anisotropy, Phys. Rev. Lett. **74**, 4503 (1995).
[77] A. Zazunov, F. Buccheri, P. Sodano, and R. Egger, 6π Josephson effect in Majorana box devices, Phys. Rev. Lett. **118**, 057001 (2017).